JOURNAL OF QUATERNARY SCIENCE (2001) **16**(7) 717–726

DOI: 10.1002/jqs.650

Holocene variations of sea-surface conditions in the southeastern Barents Sea, reconstructed from dinoflagellate cyst assemblages

ELENA VORONINA,[1]* LEONID POLYAK,[2] ANNE DE VERNAL[1] and ODILE PEYRON[1]
[1] GEOTOP, Université du Québec à Montréal, P.O. Box 8888, Montréal, Québec, H3C 3P8, Canada
[2] Byrd Polar Research Center, Ohio State University, Columbus, OH 43210, USA

Voronina, E., Polyak, L., de Vernal, A. and Peyron, O. 2001. Holocene variations of sea-surface conditions in the southeastern Barents Sea reconstructed from dinoflagellate cyst assemblages. *J. Quaternary Sci.,* **Vol. 16** pp. 717–726. ISSN 0267-8179.

Received 19 May 2001; Revised 16 July 2001; Accepted 16 July 2001

ABSTRACT: Palynomorphs were analysed in two sediment cores from the southeastern Barents Sea representing the past 8.3 and 4.4 kyr. High dinocyst contents and species diversity enabled the application of the best analogue method to quantitatively reconstruct sea-surface salinities, temperatures and ice cover using 677 modern reference sites from the North Atlantic and Arctic seas, including new data from the Barents Sea reported here. At the southern core site, where waters are affected by the Atlantic inflow, sea-surface conditions were relatively warm and stable between ca. 8000 and 5000 calendar yr BP. In contrast, the past 5 kyr had periods with cooler temperatures and extended ice cover, fluctuating mostly at 1–1.5 kyr frequencies at both sites. Most pronounced coolings occurred around 8.1, 5, 3.5–3.2 and 2.5 ka. The northern site additionally shows younger cooling events, tentatively dated to 1.4, 0.3 and 0.1 ka. Identified variations in sea-surface conditions indicate changes in Atlantic water inputs to the Barents Sea. Our results generally correlate to palaeoclimatic reconstructions from northwestern Eurasia, exemplified by palynological records from Karelia. This correlation suggests that sea-surface variations in the Barents Sea reflect large-scale changes in atmospheric and oceanic interactions between the North Atlantic and the Arctic. Copyright © 2001 John Wiley & Sons, Ltd.

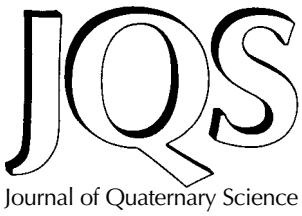

KEYWORDS: dinoflagellate cysts; Holocene; Barents Sea; palaeoceanography; sea-surface reconstructions.

Introduction

The Barents Sea is a key area for investigating interactions between the Arctic and North Atlantic oceanic systems owing to its location at the crossroads of Arctic and Atlantic waters. Upon transiting the Norwegian Sea, the North Atlantic Drift (Norwegian Current) continues as two major branches: one entering the Barents Sea from the southwest, and another flowing northwards along its western margin (Fig. 1). These two flows reach about 2 Sv ($10^6 m^3 s^{-1}$) each and control most of the heat fluxes to the Arctic Ocean (e.g. Rudels *et al.*, 1994; Zhang *et al.*, 1998). The boundary between the Atlantic and the Arctic waters in the Barents Sea, termed the Polar Front, is characterised by sharp hydrographic gradients, which favour high biological productivity. The Polar Front corresponds largely to a mean winter limit of sea ice, which is controlled by Atlantic water inflow, in contrast to the air-temperature controlled summer ice margin. The position of the winter ice limit in the western Barents Sea is fairly stable; whereas, further southeast it varies strongly on interannual and longer term time scales. Historical observations show that the winter ice limit in the southeastern Barents Sea migrates from an almost longitudinal position west of 40°E to a zonal position at 76°N (Fig. 2; e.g. Loeng, 1991). These fluctuations co vary with changes in the Atlantic water influx (Mysak and Manak, 1989; Loeng, 1991). The investigation of the past ice extents and oceanographic conditions in sedimentary records from this area will, thus, allow evaluation of variations in Atlantic water inputs to the Arctic.

Because of low sedimentation rates in the southwestern Barents Sea, affected by a high-energy flow of Atlantic water, sites suitable for high-resolution palaeoceanographic reconstruction are to be sought east and north of the winter sea-ice limit. There have been several studies of the Holocene proxy records from these areas, based mainly on benthic foraminifer assemblages and stable isotopes (Polyak and Mikhailov, 1996; Hald *et al.*, 1999; Duplessy *et al.*, 2001; Lubinski *et al.*, 2001). These results indicate noticeable variations of hydrographic conditions on millennial and sub-millennial time-scales. However, foraminiferal compositions

*Correspondence to: Elena Voronina, GEOTOP, Université du Québec à Montréal, P.O. Box 8888, Montréal, Québec, H3C 3P8, Canada.

Contract/grant sponsor: National Science and Engineering Council of Canada.
Contract/grant sponsor: National Science Foundation (USA); Contract/grant number: OPP-9725418.

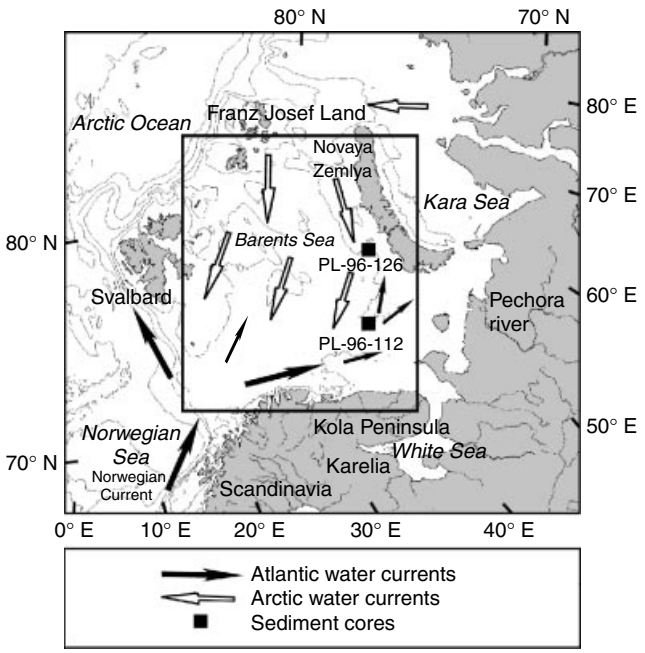

Figure 1 Map of the Barents Sea and location of coring sites PL-96-112 and PL-96-126. Water depth is shown in 200, 500, 1000, 2000 and 3000 m contour lines. The rectangle delimits the study area shown in Fig. 2

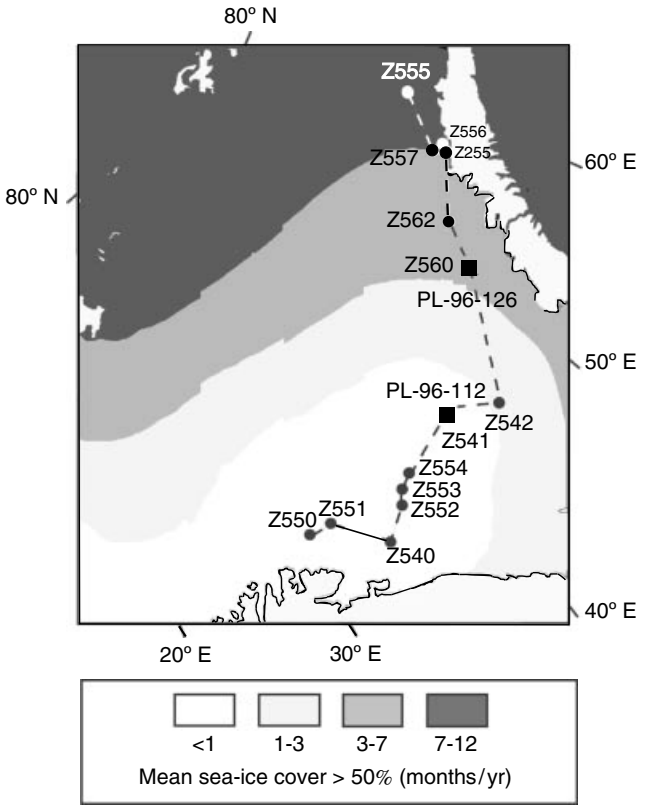

Figure 2 Location of the cores and surface sediment samples used to document the distribution of dinocyst assemblages along a southwest to northeast transect. The modern sea-ice cover extent (in months yr^{-1} with >50% of coverage) is illustrated based on the 1953–1990 data set of the National Climate Data Center

in sedimentary records are commonly distorted by dissolution or disaggregation and stable-isotope records from continental shelves are often difficult to interpret because of local hydrochemical effects. The only known palaeobiological proxy in the high-latitude seas that is resistant to taphonomic processes and provides a relatively easily interpretable record of sea-surface conditions is organic-walled dinoflagellate cysts (dinocysts) (e.g. Mudie and Short, 1985; Mudie, 1992; de Vernal *et al.*, 1994, 1997). Here, we report on dinocyst assemblages in two sediment cores from the southeastern Barents Sea that document variations in sea-surface conditions during the middle to late Holocene, i.e. the past ca. 8.3 kyr. The two cores selected, PL-96-112 and PL-96-126, are located between the modern maximum and minimum winter sea-ice limits, south and north of the mean multiyear limit, respectively (Table 1; Figs 1 and 2). This location is favourable for examining past variations in ice extent. Prevailing sediment deposition rates of over 50 cm kyr^{-1}, estimated by ^{14}C dating, allow detection of these variations on a submillennial scale. We also have investigated dinocyst assemblages in surface sediments along a southwest–northeast transect across the Barents Sea (Table 1; Fig. 2) in order to define the regional relationships with modern sea-surface conditions.

Methods

Sediment cores were collected with box and gravity corers from R/V *Professor Logachev* in 1996. For characterisation of surface sediments (0–2 cm), we have selected box-corer and grab samples from various collections along a SW–NE transect across the Barents Sea (Fig. 2). Results of dinocyst counts in surface sediments are included into the North Atlantic–Arctic data base (de Vernal *et al.*, this issue) and only summarised data are presented here. Subsampling of cores for palynology was done mostly at 10-cm intervals. Sediment samples of 5 cm^3 were processed for palynological analyses following the standard procedure used at GEOTOP (de Vernal *et al.*, 1999; Rochon *et al.*, 1999). Palynomorph concentrations were evaluated on the basis of the marker-grains method (Matthews, 1969), which yields results accurate to about 10% for a 0.95 confidence interval (de Vernal

Table 1 Location of sediment cores and surface sediment samples

Station Number	Sampling type	Latitude N	Longitude E	Water depth (m)
PL-96-112 G	Gravity core	71°44.2′	42°36.3′	286
PL-96-126 G	Gravity core	73°37.5′	50°43.0′	270
Z555	Grab	76°43.1′	59°46.0′	303
Z557	Grab	75°37.0′	56°26.0′	175
Z556	Grab	75°26.0′	57°19.0′	143
Z255	Core top	75°23.4′	57°23.9′	140
Z562	Box core	74°27.2′	52°25.8′	250
Z560	Box core	73°37.4′	50°43.6′	274
Z542	Box core	71°07.0′	45°14.9′	266
Z541	Box core	71°44.2′	42°36.7′	286
Z553	Grab	71°04.1′	37°02.7′	220
Z554	Grab	71°15.6′	37°54.8′	282
Z552	Grab	70°49.6′	36°15.7′	160
Z540	Box core	70°20.6′	34°22.0′	263
Z551	Grab	71°23.5′	31°58.4′	245
Z550	Grab	71°24.8′	30°24.7′	280

et al., 1987). Wet sieving through 10 and 120 µm mesh sieves was undertaken in order to remove coarse sand and fine silt and clay particles. The 10–120 µm fraction was treated repeatedly with HCl (10%) and HF (49%) to dissolve carbonate and silica particles. After a final sieving at 10 µm, the residue was mounted between a slide and cover slide in glycerine gel.

Recovered palynomorphs were identified and counted using a transmitted-light microscope under ×400 or ×1000 magnification. Palynomorphs included mainly cysts of dinoflagellates, which live in the upper water column, but also pollen and spores of terrestrial origin, as well as organic linings of benthic foraminifers. Ancient palynomorphs were distinguished on the basis of the diagenetic alteration of the membrane; their presence indicates erosion and redeposition of pre-Quaternary sediments. Here, we present concentrations of the major palynomorph groups with a special attention to dinocysts, which were identified to species level using the taxonomical nomenclature described by Head in Rochon *et al.* (1999). We also use the updated taxonomical nomenclature for the new genus *Islandinium*, including the species *I. minutum* and *I.*? *cezare*, which were known previously as *Algidasphaeridium*? *minutum* var. *minutum* and *Algidasphaeridium*? *minutum* var. *cezare* (cf. Head *et al.*, this issue). One of the most abundant dinocysts in the Barents Sea assemblages, *Operculodinium centrocarpum*, exhibits large morphological variations, with many specimens having only few and imperfectly developed processes, distributed unevenly around the cyst. These specimens were designated under the name of *O. centrocarpum*—arctic morphotype (cf. de Vernal *et al.*, this issue; Radi *et al.*, this issue). In all samples, a minimum of 300 dinocysts were identified and counted to calculate taxa percentages. Our counts were added to the reference dinocyst data base including 677 data points (de Vernal *et al.*, this issue) and were used to reconstruct sea-surface conditions in the southeastern Barents Sea by means of the best analogue method (cf. Guiot, 1990). Data treatment was undertaken using the PPP-base software of Guiot and Goeury (1996) following the procedures described by de Vernal *et al.* (this issue). Reference modern multi-annual temperatures and salinities were compiled from the National Ocean Data Center data base (NODC, 1994); ice-extent values (in months yr^{-1} with >50% of coverage) are based on the 1953–1990 data set of the National Climate Data Center.

Distribution of dinocysts in surface sediments of the Barents Sea

Surface sediment samples from the southern, mostly ice-free part of the transect (Fig. 2) reveal abundant dinocysts with concentrations reaching 525 000 cysts cm^{-3} (Fig. 3). These abundances possibly indicate high productivity in the upper water column, consistent with phytoplankton observations (e.g. Rey and Loeng, 1985). Additionally, redistribution of fine sediment by currents results in locally reduced or enriched palynomorph concentrations. The dinocyst assemblages in the southern part of the transect are dominated by *Operculodinium centrocarpum* sensu Wall and Dale 1966, *Nematosphaeropsis labyrinthus*, and the cyst of *Pentapharsodinium dalei*. In the more northern part of the Barents Sea, which is covered by Arctic surface water with seasonal ice cover in winter and relatively low salinity in summer, the dinocyst assemblages have lower percentages of *O. centrocarpum* sensu Wall and Dale 1966 and significant percentages of *Islandinium minutum*. Samples Z556 and Z255, located in or near the fjords of Novaya Zemlya affected by glacier meltwater, are further characterised by elevated percentages of *Brigantedinium* spp. *Islandinium minutum* and *Brigantedinium* spp., both belonging to the order Peridiniales, have been inferred to relate to a heterotrophic production (e.g. Jacobsen and Anderson, 1986).

The zonation of dinocyst assemblages in the Barents Sea is illustrated by the principal component analysis. Component 1 (PC1) corresponds to an opposition between *Brigantedinium* and *Islandinium* and the other taxa, notably *Operculodinium centrocarpum*; it explains 44% of the variance and appears to be associated with reduced ice cover and to elevated temperature and salinity. The characteristically high content of supposedly heterotrophic dinocysts in Arctic-water assemblages may be linked with the domination of the Arctic autotrophic phytoplankton by diatoms (Nesvetova and Ryzhov, 1987). Abundant diatoms constitute a feeding source for heterotrophic organisms and also compete with autotrophic dinoflagellate taxa.

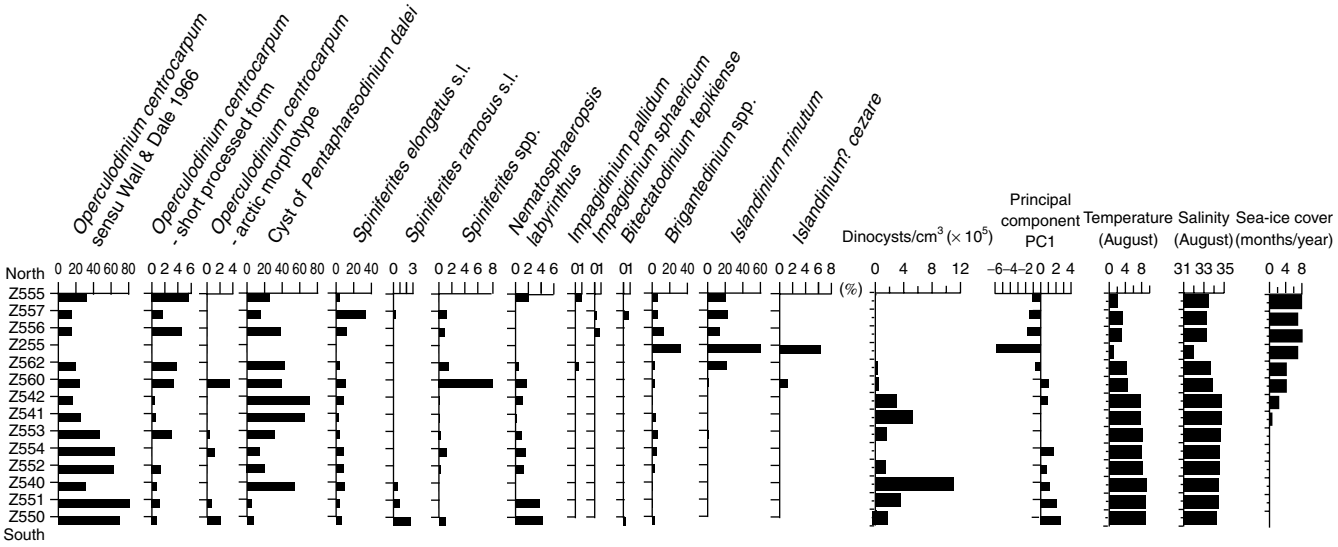

Figure 3 Diagram of dinocyst taxa percentages in surface sediment samples from the southwest to northeast transect (Fig. 2), corresponding principal component values (PC1), and multi-annual modern sea-surface temperature, salinity and sea-ice cover. Temperatures and salinities were compiled from the National Ocean Data Center data set (NODC, 1994), and the sea ice cover is from the National Climate Data Center

Stratigraphy of sediment cores

Cores PL96-112 and PL96-126 consist of clayey–silty mud with <10% sand, relatively high total organic carbon content (1–3%), and low calcium carbonate content (below 2%), consistent with the composition of modern sediments in the study area (Wright, 1974). The biogenic component in the sand fraction is sparse: planktonic foraminifers are very rare and benthic foraminifers occur in low to moderate numbers (up to 100 test g^{-1}). In a few samples, mollusc shell debris and calcareous benthic foraminiferal tests permitted ^{14}C measurements by accelerator mass spectrometry (Table 2). The ^{14}C ages were corrected by 460 yr to account for the air–sea reservoir difference, including 60-yr local correction for the Barents Sea (Stuiver and Braziunas, 1993). Calibration to calendar years was made using the software CALIB 4.3 for marine carbonate (Stuiver *et al.*, 1998, 2000). The ages obtained indicate that cores PL-96-112 and PL-96-126 span ca. 8.3 and 4.4 kyr, respectively, with sedimentation rates ranging mostly from 20 to 100 cm kyr^{-1} in PL-96-112 and 60 to 120 cm kyr^{-1} in PL-96-126. Thus, palynological analysis performed at a 10-cm interval characterises Holocene palaeoceanographic conditions with a submillennial to century-scale resolution. Age models were constructed by interpolation between the dated points (Fig. 4). Core tops were assumed to represent modern age, which provides only tentative age control for the upper part of gravity cores because of a possible loss of uppermost sediments in the coring process. However, this age model for PL-96-112 proved to be accurate, as verified by a ^{14}C age from the accompanying box core (Table 2; Fig. 4).

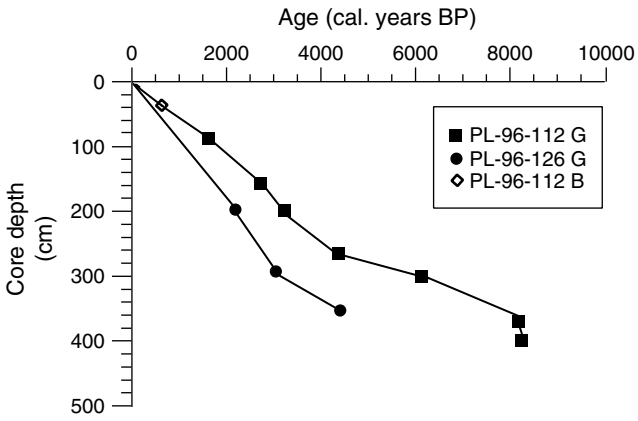

Figure 4 Age–depth relationship for cores PL-96-112 (G and B) and PL-96-126 (G)

Palynological records and the reconstruction of Holocene sea-surface conditions

Both cores PL-96-112 and PL-96-126 are rich in palynomorphs, with dinocyst concentrations in the order of 10^4 to 10^5 cm^{-3}, reaching maximum values in PL-96-112 during the past ca. 3.5 ka (Figs 5 and 6). These numbers correspond to fluxes ranging from 10^2 to 10^4 cysts cm^{-2} yr^{-1}, among the highest recorded in recent sediments from high latitudes (e.g. de Vernal *et al.*, 1994, 1997; Rochon and de Vernal, 1994). Dinocyst concentrations are controlled by productivity in the upper water column and by sedimentation processes. Because composition of sediment in cores PL-96-112 and PL-96-126 does not reveal strong down-core changes, we believe that dinocyst abundances reflect mainly biological productivity. Additionally, the organic linings of foraminifers ranging in concentrations between 1 000 and 20 000 cm^{-3} indicate a high benthic production and pollen and spore concentrations of the 10^3 to 10^4 cm^{-3} reflect significant inputs from the terrestrial vegetation of adjacent land. The palynomorph concentrations are generally lower in core PL-96-126 than in core PL-96-112, probably because of lower productivity at the more northern site and/or stronger dilution by clastic sediment.

The dinocyst assemblages of cores PL-96-112 and PL-96-126 are dominated by *Operculodinium centrocarpum* sensu Wall and Dale 1966, *Pentapharsodinium dalei* cysts, and

Table 2 AMS ^{14}C ages for cores PL-96-112 G and B and PL-96-126 G. A correction of 460 yr has been applied to account for the air–sea reservoir difference. The calibrated ages were calculated using the software CALIB 4.3 (Stuiver *et al.*, 1998, 2000)

Laboratory number	Core	Depth in core (cm)	Material dated	^{14}C age	Corrected ^{14}C age	Calibrated yr BP
AA34306	PL-96-112 B	37.5	Benthic foraminifers	1140 ± 60	680	645
AA35040	PL-96-112 G	91	*Dentalium* spp.	1980 ± 70	1520	1477
AA34307	PL-96-112 G	156	Shell debris	2955 ± 45	2495	2702
AA35041	PL-96-112 G	206	*Nuculana pernula*	3445 ± 50	2985	3253
AA35042	PL-96-112 G	271	*Bathyarca glacialis*	4190 ± 60	3730	4175
AA34308	PL-96-112 G	309.5	Shell debris	5820 ± 55	5360	6178
AA34309	PL-96-112 G	376	*Astarte* spp.	7775 ± 60	7315	8164
AA25446	PL-96-112 G	406	Benthic foraminifers and shell debris	7885 ± 70	7425	8305
AA35044	PL-96-126 G	203	*Nuculoma tenuis*	2545 ± 45	2085	2126
AA39574	PL-96-126 G	294	Shell debris	3326 ± 57	2866	3000
AA34310	PL-96-126 G	353	Benthic foraminifers	4315 ± 50	3855	4375

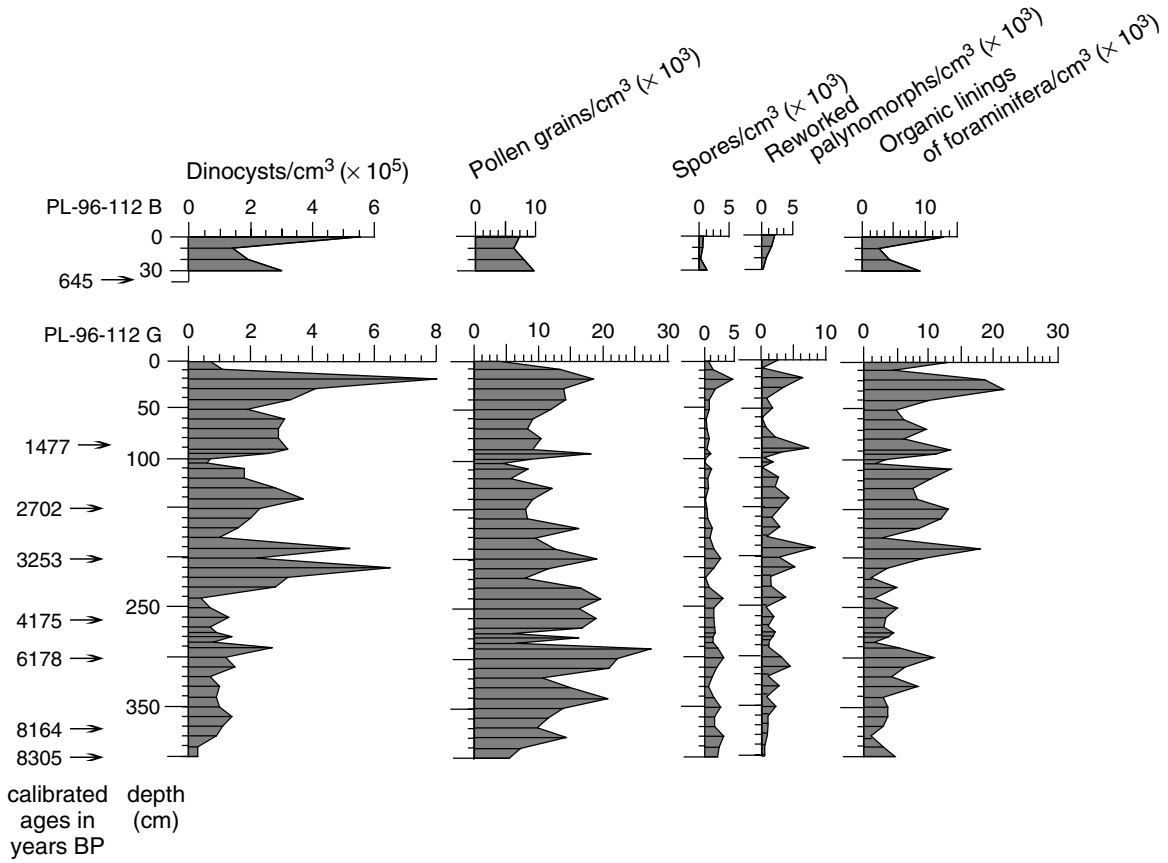

Figure 5 Palynomorph concentrations in the gravity (G) and box (B) cores PL-96-112. The ages are shown to the left of the diagram in calibrated years (Table 2)

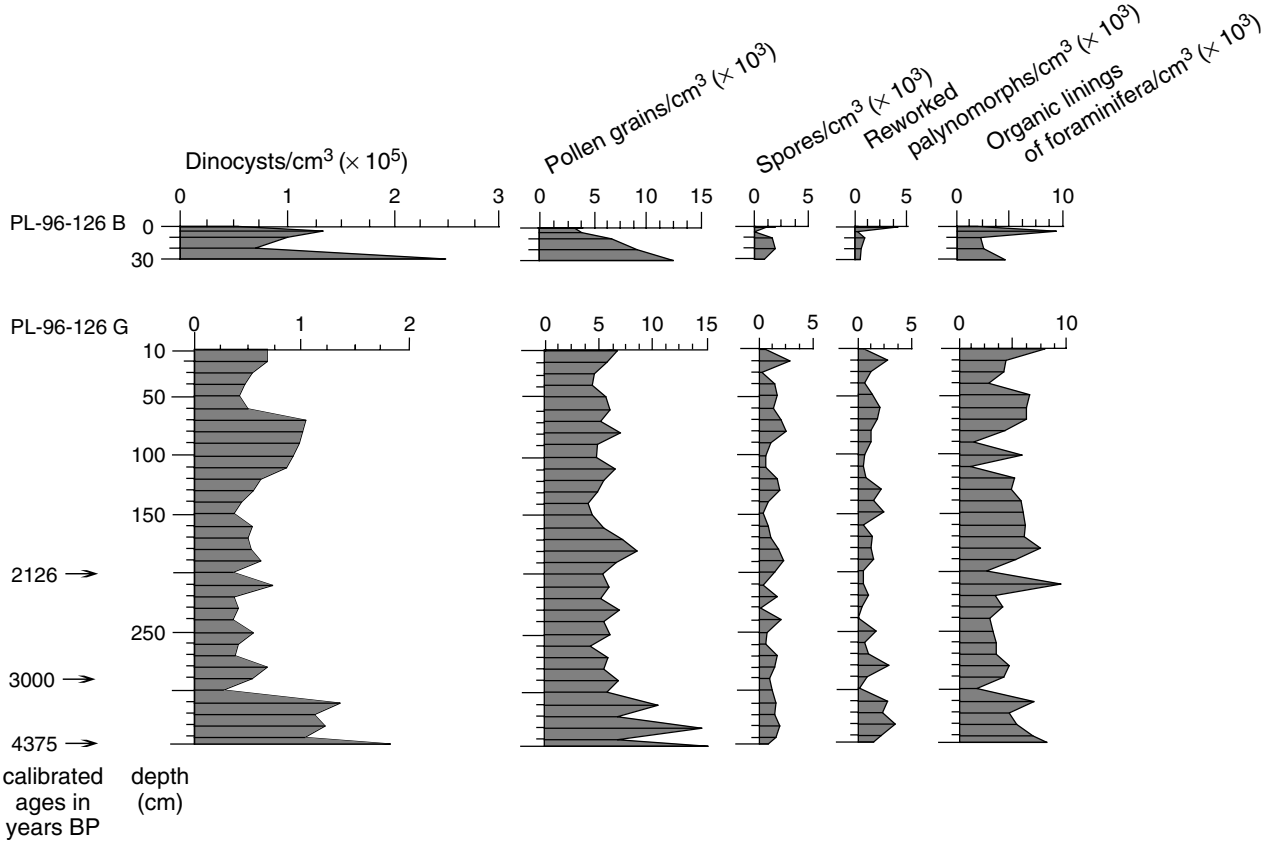

Figure 6 Palynomorph concentrations in the gravity (G) and box (B) cores PL-96-126. The ages are shown to the left of the diagram in calibrated years (Table 2)

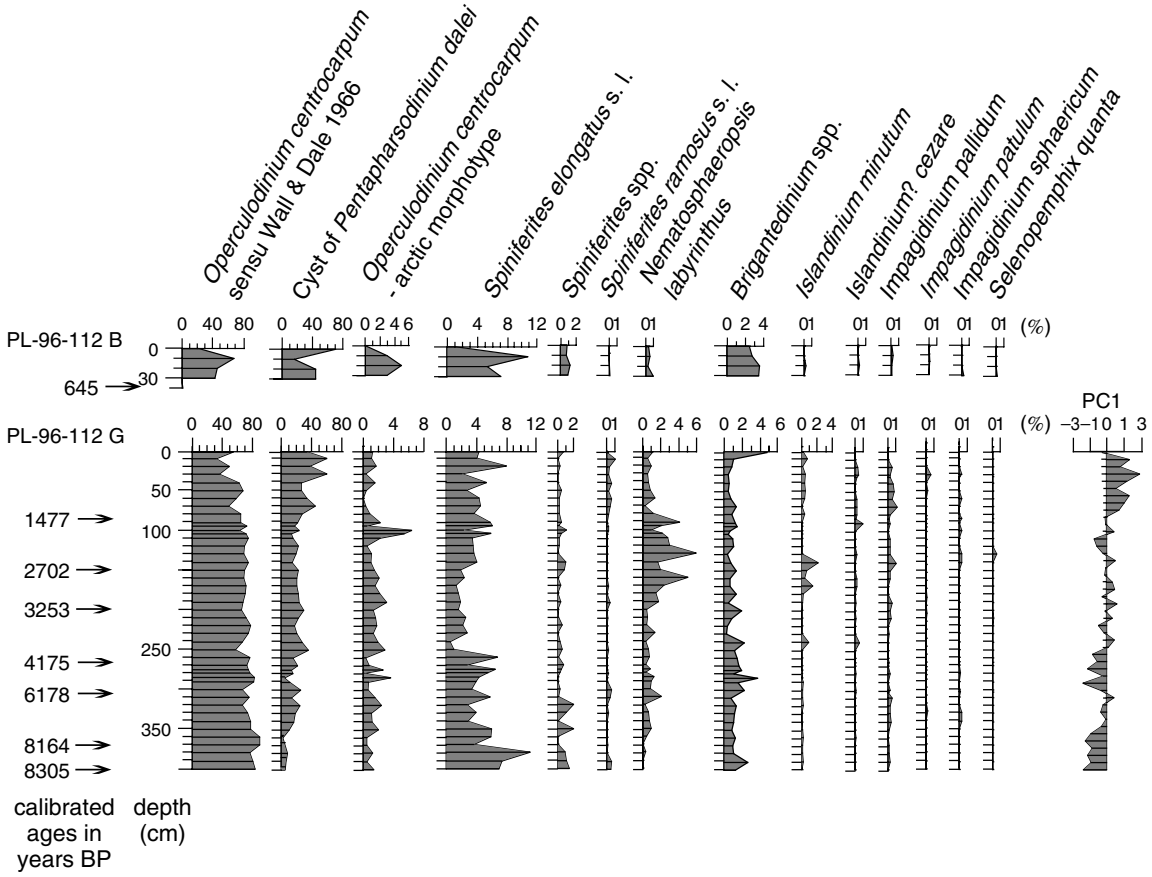

Figure 7 Dinocyst taxa percentages in the gravity (G) and box (B) cores PL-96-112. The ages are expressed in calibrated years (Table 2)

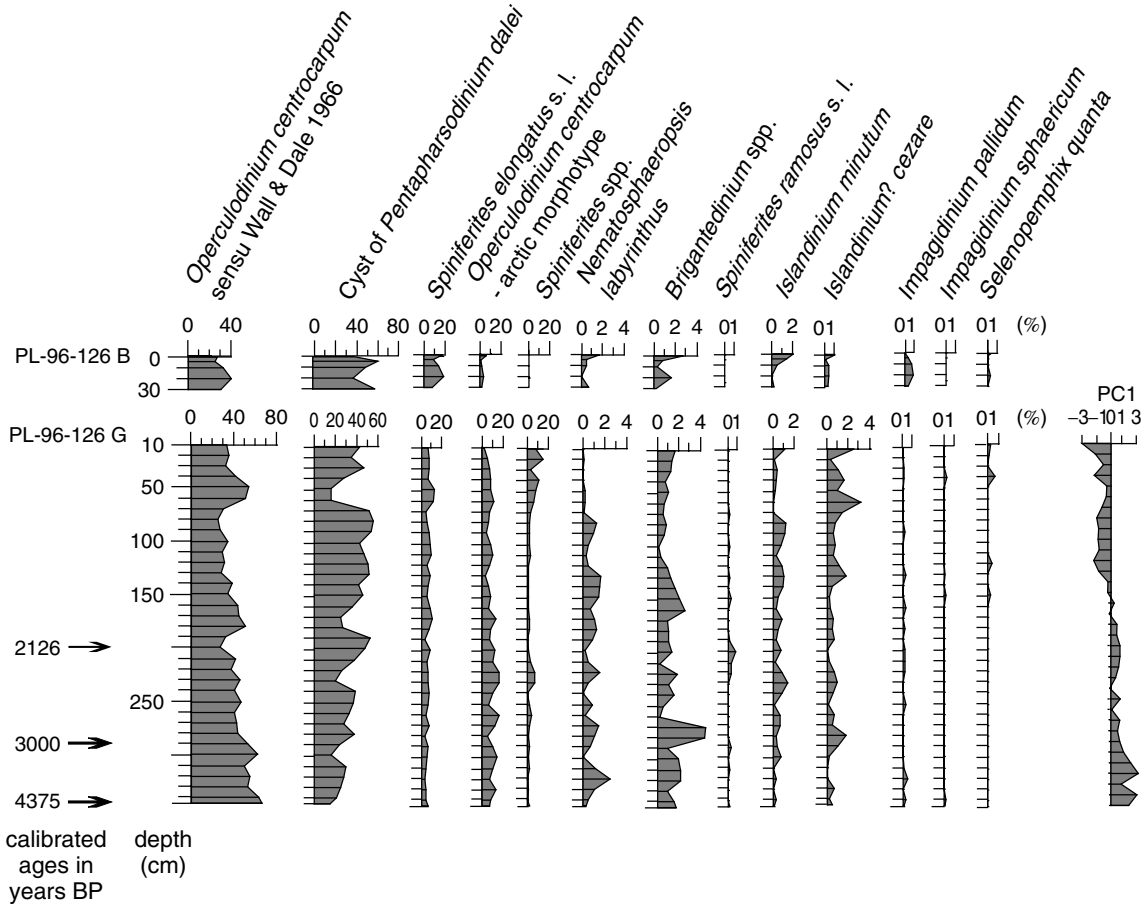

Figure 8 Dinocyst taxa percentages in the gravity (G) and box (B) cores PL-96-126. The ages are expressed in calibrated years (Table 2)

Spiniferites elongatus s.l., which are accompanied mainly by *Nematosphaeropsis labyrinthus* and *Brigantedinium* spp. (Figs 7 and 8). Despite a general similarity in species composition, the dinocyst assemblages of the two cores show some distinctly differing features. In particular, the percentages of *O. centrocarpum* are higher in core PL-96-112, whereas *Islandinium minutum* and *Islandinium*? *cezare* are more abundant in core PL-96-126, consistent with the more southern location of core PL-96-112.

Dinocyst assemblages in core PL-96-112 are largely similar to the modern assemblages from the southern Barents Sea and vary only moderately in the percentages of main taxa (Fig. 7). The most distinct up-core change is the increase in percentage of *Pentapharsodinium dalei* cysts at the expense of *Operculodinium centrocarpum*. This trend, highlighted by the principal component analysis, suggests a generally closer position of the Polar Front to the core site in the younger part of the record. The reconstruction of sea-surface conditions using the best analogue method indicates generally warm August sea-surface temperatures, mostly within the modern range of 7.8 ± 1.9°C (NODC, 1994), and limited ice cover throughout most of the past 8 kyr (Fig. 9). Nevertheless, the record displays recurring episodes of lowered temperatures and salinities and increased ice extent, notably at ca. 8.1, 5.0, 3.5 and 2.5 cal. ka.

As in core PL-96-112, dinocyst assemblages in core PL-96-126 show little variation in main taxa percentages (Fig. 8), being generally similar to modern assemblages from the northern Barents Sea as well as many sites in the western Arctic and Bering Sea (Radi *et al.*, this issue) or the Hudson Bay (e.g. Rochon *et al.*, 1999). The percentages of the cyst of *P. dalei* also generally increase concomitant with a decrease in *Operculodinium centrocarpum* towards the top of PL-96-126. The reconstruction of sea-surface conditions (Fig. 10) suggests that during the past 4.4 kyr sea-ice cover at this site developed mostly for 2–3 months yr^{-1} on average, less than the modern mean of 4.3 months yr^{-1}. The August temperature generally ranged between 6 and 8°C, slightly warmer values than at present (4.6°C; NODC, 1994). However, episodes of more extensive sea-ice cover, up to 6 months yr^{-1}, accompanied by lowered temperatures and salinities, developed during intervals centred around approximately 3.2, 2.5, 1.4, 0.3 and 0.1 cal. ka. The latter three ages are tentative because of insufficient age control for the upper part of the core.

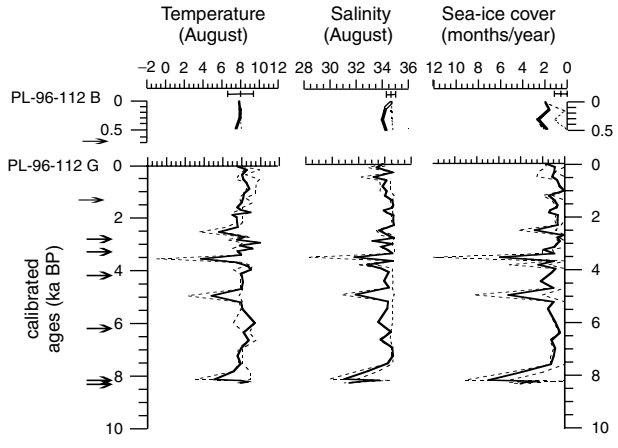

Figure 9 Reconstruction of sea-surface conditions from dinocyst distribution in gravity (G) and box (B) cores PL-96-112 against age. Solid lines represent the most probable reconstructed values (weighted averages of the five best analogues) within a confidence interval delimited by minimum and maximum values (dotted lines) from the five best analogues. The chronology is based on interpolations between calibrated ages (Table 2). Arrows to the left show position of ^{14}C dates. Bars on top show multi-annual modern values of temperature, salinity and ice extent: mean values (central lines) and dispersions (1σ)

Discussion

The dinocyst records in both PL-96-112 and PL-96-126 indicate relatively warm surface waters and limited ice extent, and thus a significant influx of Atlantic water into the southeastern Barents Sea during most of the middle and late Holocene spanning the past ca. 8.3 kyr (Figs 9 and 10). Especially stable and warm conditions are reconstructed for PL-96-112 between 8 and 5 cal. ka. This time interval has been characterised by generally warm, but gradually deteriorating oceanic and climatic conditions in the Barents Sea (Polyak and Mikhailov, 1996; Lubinski *et al.*, 1999) as well as in the western part of the Nordic seas (Koç *et al.*, 1993). The oldest part of this period was marked by maximal Atlantic water inputs to the northern margin of the Barents Sea, which may indicate either an overall increase in Atlantic fluxes with the Norwegian Current or a preferential intensification of its northern branch (Duplessy *et al.*, 2001; Lubinski *et al.*, 2001). The PL-96-112 data do not reveal variations within the 8–5 ka interval, possibly because the Polar Front was consistently located north of the site, but show a distinct preceding cooling pulse dated to ca. 8.1 cal. ka. This age is close, although may not match exactly, the widespread '8.2 ka' cooling event detected in many high-latitude locations, especially around the North Atlantic (e.g. Alley *et al.*, 1997; Barber *et al.*, 1999). A correlative cooling has been inferred for the northern margin of the Barents Sea (Duplessy *et al.*, 2001), thus suggesting an overall decrease in Atlantic water inputs to the Arctic Ocean. More records with a detailed chronostratigraphical control are needed to evaluate the effect of this cooling event on the Arctic.

A significant change in the hydrographic regime in the southeastern Barents Sea occurred at approximately 5 cal. ka, as reflected in PL-96-112. Sea-surface conditions became less stable than during the preceding 3 kyr and featured several cooling pulses, notably around 5.0, 3.5 and 2.5 cal. ka in PL-96-112 and at 3.2, 2.5, 1.4, 0.3 and 0.1 cal. ka in PL-96-126

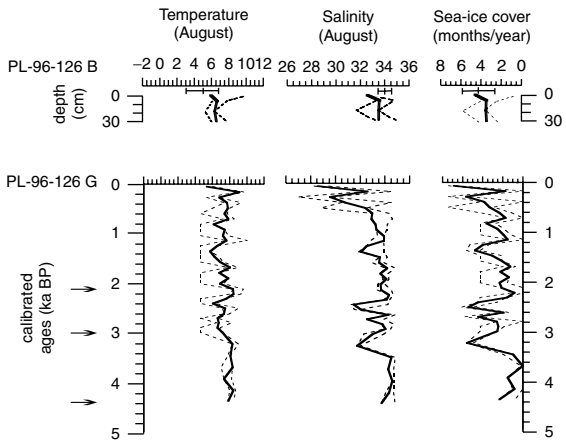

Figure 10 Reconstruction of sea-surface conditions from dinocyst distribution in gravity (G) and box (B) cores PL-96-126 against age and core depth, respectively. See caption to Fig. 9 for more explanation

(the three latter ages are tentative). The transition to cooler and fluctuating environments in PL-96-112 is marked by a fourfold increase in sedimentation rates, possibly reflecting higher sediment fluxes from the extended ice cover. Foraminiferal data also suggest a southward migration of the Polar Front at or soon after approximately 5 ka (Polyak and Mikhailov, 1996), consistent with the establishment of generally cool conditions in the Nordic seas (Koç *et al.*, 1993). Simultaneously, at the northern Barents Sea margin, the eastward propagation of Atlantic water developed a stronger gradient, possibly owing to a weakening of Atlantic inputs (Lubinski *et al.*, 2001 in press).

Our records of sea-surface conditions show a good correspondence to palaeobotanical data from adjacent land for the past ca. 8 kyr, when a generally modern-type palaeogeographical setting was established after the completion of deglaciation and major sea-level rise (cf. Stager and Mayewski, 1997). The warm interval identified in PL-96-112 between 8 and 5 cal. ka correlates to the maximal forest expansion in northern Eurasia, whereas the unstable and generally cooler subsequent period with extended sea-ice cover corresponds to forest retreat, although the age of the transition is slightly diachronous (e.g. Andreev and Klimanov, 2000; MacDonald *et al.*, 2000). A comparison of our sea-surface reconstructions with palynology based palaeoclimatic records from Karelia, well south of the Barents Sea (Fig. 1; Klimanov and Elina, 1984; Velichko *et al.*, 1997), suggests a correlation of not only major trends, but also of finer scale climatic variations during the past ca. 8 kyr (Fig. 11). This correlation, which still needs to be verified by more records with rigorous age control, implies a strong climatic linkage between the northwestern Eurasia and the Barents Sea during much of the Holocene. Such linkage can be explained by a coupling of atmospheric and oceanic heat fluxes from the North Atlantic, which affect the vegetation in northwestern Eurasia and the sea-ice extent in the Barents Sea, respectively.

The shift towards a colder climate in northern high latitudes 4–5 kyr ago has been interpreted to result from a decrease in summer insolation (e.g., Kutzbach *et al.*, 1993). The accompanying decrease in seasonality could have reduced the atmospheric transport from the North Atlantic to Eurasia and, thus, the Atlantic water drift, which would allow winter sea-ice in the Barents Sea to expand southwards. The pervasive nature of this transition around the North Atlantic is exemplified by contemporaneous oceanographic changes at the eastern Greenland margin (Jennings *et al.*, 2000) and in the Skagerrak–Kattegat area (Conradsen and Heier-Nielsen, 1995; Jiang *et al.*, 1997).

During the warm interval between ca. 8 and 5 cal. ka, variations in the strength of Atlantic inputs are not revealed at the PL-96-112 site and probably should be sought for in the more northern areas. However, it is also possible that climatic conditions around the North Atlantic were genuinely more stable during periods of stronger northwards drift of Atlantic water (Alley *et al.*, 1999). During the subsequent period of generally colder climate, cooling pulses, presumably associated with a decrease in Atlantic water fluxes, are evident in both cores studied, mostly at 1.5 to 1 kyr intervals. This frequency suggests a possible link to millennial oscillations recorded in sedimentary sequences in and around the North Atlantic (e.g., Bond *et al.*, 1997; Bianchi and McCave, 1999). More studies on records with rigorous age control and a submillennial resolution are needed from the Barents Sea region to conclude on the nature of oceanic–climatic interactions downstream of the North Atlantic drift.

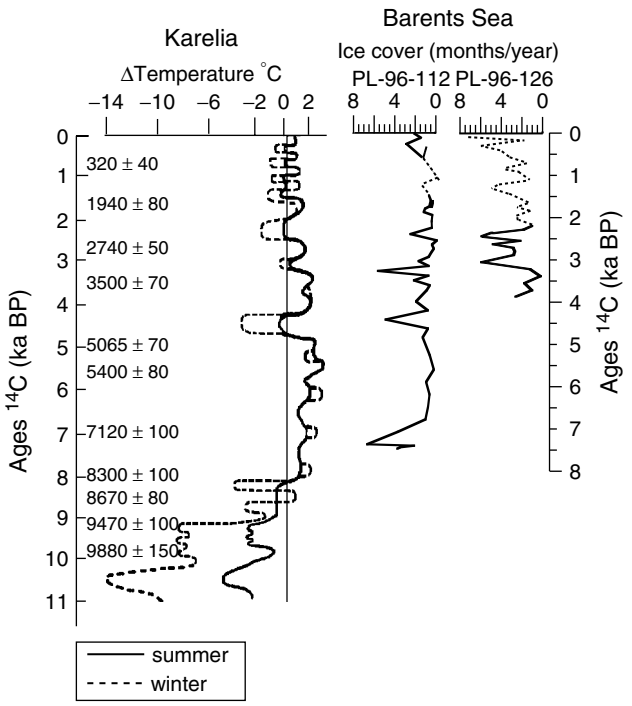

Figure 11 Comparison between the composite terrestrial palaeoclimatic reconstruction from Karelia (left panel; Klimanov and Elina, 1984; Velichko *et al.*, 1997) and the mean ice extent at the sites of PL-96-112 and PL-96-126 in the southeastern Barents Sea reconstructed from dinocyst assemblages (right panel; Figs 9 and 10). Reconstructions above the uppermost dated levels in gravity cores are shown by dotted lines; box-core data are shown for PL-96-112. In the left panel, solid and dashed lines represent summer and winter temperature deviations from modern values, respectively

Conclusions

Dinocyst assemblages from surface sediments in the Barents Sea show distinct changes along a southwest–northeast transect. Southern assemblages, from ice-free waters affected by Atlantic fluxes, are characterised by very high percentages of *Operculodinium centrocarpum* sensu Wall and Dale 1966 and significant amounts of *Nematosphaeropsis labyrinthus* and the cyst of *Pentapharsodinium dalei*. The abundance of the cyst of *P. dalei* increases near high-productivity waters of the Polar Front, corresponding to the mean winter sea-ice margin. Further north, under the seasonal ice cover, dinocysts have elevated percentages of *Islandinium*? *cezare*, *Islandinium minutum* and *Brigantedinium* spp., the latter being especially characteristic for sites affected by glacier meltwater discharge from Novaya Zemlya.

Distribution of dinocysts in two age-constrained sediment cores from the southeastern Barents Sea was used for proxy reconstructions of sea-surface salinities, temperatures and ice cover for much of the Holocene, i.e. the past 8.3 and 4.4 kyr. According to our reconstructions, environments were relatively warm and stable during the period from approximately 8 to 5 cal. ka. This interval was preceded by a cold spike at ca. 8.1 ka, possibly correlative to a '8.2 ka' cooling event widely recognised around the North Atlantic. After 5 ka, several episodes of decreased temperatures and expanded ice cover occurred in the southeastern Barents Sea, notably at 5, 3.5–3.2 and 2.5 cal. ka. Additionally, three younger cooling events are identified in the northern core, with ages estimated tentatively as 1.4, 0.3 and 0.1 ka. Our reconstructed

sea-surface characteristics match the palaeoclimatic variations inferred from palynological data from northwestern Eurasia. Notably, warm 8 to 5 ka conditions and the cooler and less stable subsequent period are consistent on land and in the Barents Sea, and even some short-term events appear to be correlative in terrestrial and marine records. These data indicate a strong linkage between the climatic and oceanic processes driven by atmospheric and water inputs from the North Atlantic, respectively. The Holocene climate in the Atlantic sector of the Arctic presumably was controlled by a combination of changes in insolation and variations in North Atlantic fluxes.

Acknowledgements This study was supported by the National Science and Engineering Council of Canada, notably through the network project Climate System History and Dynamics (CSHD) to A. de Vernal, and by the USA National Science Foundation award OPP-9725418 to L. Polyak. We are grateful to Maryse Henry and Virginie Loucheur for their help in laboratory work. The comments by the reviewers, Jens Matthiessen and Jochen Knies, were very helpful in improving the manuscript.

References

Alley RB, Mayewski PA, Sowers T, Stuiver M, Taylor KC, Clark PU. 1997. Holocene climatic instability: a prominent, widespread event 8200 yr ago. *Geology* **25**: 483–486.

Alley RB, Mayewski PA, Saltzman ES. 1999. Increasing North Atlantic climate variability recorded in a central Greenland ice core. *Polar Geography* **23**: 119–131.

Andreev A, Klimanov V. 2000. Quantitative Holocene climatic reconstruction from Arctic Russia. *Journal of Palaeolimnology* **24**: 81–91.

Barber DC, Jennings AE, Andrews JT, Kerwin MW, Morehead MD, Dyke A, McNeely R, Hillaire-Marcel C, Bilodeau G, Southon J, Gagnon J-M. 1999. Forcing of the cold event of 8,200 years ago by catastrophic drainage of Laurentide lakes. *Nature* **400**: 344–348.

Bianchi GG, McCave IN. 1999. Holocene periodicity in North-Atlantic climate and deep-ocean flow south of Iceland. *Nature* **397**: 515–517.

Bond G, Showers W, Cheseby M, Lotti R, Almasi P, deMenocal P, Priore P, Cullen H, Hajdas I, Bonani G. 1997. A pervasive millennial-scale cycle in North Atlantic Holocene and glacial climates. *Science* **278**: 1257–1266.

Conradsen K, Heier-Nielsen S. 1995. Holocene palaeoceanography and palaeoenvironments of the Skagerrak-Kattegat, Scandinavia. *Palaeoceanography* **10**: 801–813.

De Vernal A, Larouche A, Richard PJH. 1987. Evaluation of palynomorph concentrations: do the aliquot and the marker-grain methods yield comparable results? *Pollen et Spores* **XXIX**: 291–304.

De Vernal A, Turon J-L, Guiot J. 1994. Dinoflagellate cyst distribution in high-latitude marine environments and quantative reconstruction of sea-surface salinity, temperature, and seasonality. *Canadian Journal of Earth Sciences* **31**: 48–62.

De Vernal A, Rochon A, Turon J-L, Matthiessen J. 1997. Organic-walled dinoflagellate cysts: palynological tracers of sea-surface conditions in middle to high latitude marine environments. *GEOBIOS* **30**: 905–920.

De Vernal A, Henry M, Bilodeau G. 1999. *Technique de préparation et d'analyse en micropaléontologie*. Unpublished Report, Les Cahiers du GEOTOP, Université du Québec à Montréal, 3.

De Vernal A, Henry M, Matthiessen J, Mudie PJ, Rochon A, Boessenkool K, Eynaud F, Grøsfjeld K, Guiot J, Hamel D, Harland R, Head MJ, Kunz-Pirrung M, Levac E, Loucheur V, Peyron O, Pospelova V, Radi T, Turon J-L, Voronina E. 2001. Dinoflagellate cyst assemblages as tracers of sea-surface conditions in the northern North Atlantic, Arctic and sub-Arctic seas: the new '$n = 677$' data base and application for quantitative palaeoceanographic reconstruction. *Journal of Quaternary Science* **16**: 681–698.

Duplessy J-C, Ivanova E, Murdmaa I, Paterne M, Labeyrie L. 2001. Holocene palaeoceanography of the northern Barents Sea and variations of the northward heat transport by the Atlantic Ocean. *Boreas* **30**: 2–16.

Guiot J. 1990. Methodology of palaeoclimatic reconstruction from pollen in France. *Palaeogeography, Palaeoclimatology, Palaeoecology* **80**: 49–69.

Guiot J, Goeury C. 1996. PPPbase, a software for statistical analysis of palaeoecological data. *Dendrochronologia* **14**: 295–300.

Hald M, Kolstad V, Polyak L, Forman SL, Herlihy FA, Ivanov G, Nescheretov A. 1999. Late-glacial and Holocene palaeoceanography and sedimentary environments in the St. Anna Trough, Eurasian Arctic Ocean margin. *Palaeogeography, Palaeoclimatology, Palaeoecology* **146**: 229–249.

Head MJ, Harland R, Matthiessen J. 2001. Cold marine indicators of the late Quaternary: the new dinoflagellate cyst genus *Islandinium* and related morphotypes. *Journal of Quaternary Science* **16**: 621–636.

Jacobsen DM, Anderson DM. 1986. Thecate heterotrophic dinoflagellates: feeding behavior and mechanisms. *Journal of Phycology* **34**: 153-162;

Jennings A, Knudsen K-L, Hald M, Smith LM. 2000. Mid-Holocene shift in Arctic sea ice variability on the east Greenland shelf. In *Sea Ice in the Climate System. The Record of the North Atlantic Arctic*. Abstract volume, CAPE-ICAPP Conference, Iceland; 32–33.

Jiang H, Björck S, Knudsen K-L. 1997. A palaeoclimatic and palaeoceanographic record of the last 11 000 ^{14}C years from the Skagerrak–Kattegat, northeastern Atlantic margin. *The Holocene* **7**: 301–310.

Klimanov V, Elina G. 1984. Climatic changes in northwest of Russian Plain during the Holocene. *Doklady Akademii Nauk SSSR* **274**: 1163–1166. (In russian.)

Koç N, Jansen E, Haflidason H. 1993. Palaeoceanographic reconstructions of surface ocean conditions in the Greenland, Iceland and Norwegian Seas through the last 14 ka based on diatoms. *Quaternary Science Reviews* **12**: 115–140.

Kutzbach JE, Guetter PJ, Behling PJ, Selin R. 1993. Simulated climatic changes: results of the COHMAP climate-model experiments. In *Global Climate since the Last Glacial Maximum*, Wright HE Jr, Kutzbach JE, Webb T III, Ruddiman WF, Street-Perrot FA, Bartlein PJ (eds). University of Minnesota Press: Minneapolis; 24–93.

Loeng H 1991. Features of the physical oceanographic conditions of the Barents Sea. *Polar Research* **10**: 5–18.

Lubinski DJ, Forman SL, Miller GH. 1999. Holocene glacier and climate fluctuations on Franz Josef Land, Arctic Russia, 80°N. *Quaternary Science Reviews* **18**: 85–108.

Lubinski DA, Polyak L, Forman SL. 2001. Freshwater and Atlantic Water inflows to the deep northern Barents and Kara seas since ca. 13 ^{14}C ka: foraminifera and stable isotopes. *Quaternary Science Reviews* in press.

MacDonald GM, Velichko AA, Kremenetski CV, Borisova OK, Goleva AA, Andreev AA, Cwynar LC, Riding RT, Forman SL, Edwards TWD, Aravena R, Hammarlund D, Szeicz JM, Gataullin VN. 2000. Holocene treeline history and climate change across northern Eurasia. *Quaternary Research* **53**: 302–311.

Matthews J. 1969. The assessment of a method for the determination of absolute pollen frequencies. *New Phytologist* **68**: 161–166.

Mudie PJ. 1992. Circum-Arctic Quaternary and Neogene marine palynofloras: palaeoecology and statistical analysis. In *Neogene and Quaternary Dinoflagellate Cysts and Acritarchs*, Head MJ, Wrenn JH (eds). American Association of Stratigraphic Palynologists Foundation: Dallas; 347–390.

Mudie PJ, Short SK. 1985. Marine palynology of Baffin Bay. In *Quaternary Environments*, Andrews JT (ed.). Allen & Unwin: Boston, London, Sydney; 263–308.

Mysak LA, Manak DK. 1989. Arctic sea-ice extent and anomalies, 1953-1984. *Atmosphere-Ocean* **27**: 376–405.

Nesvetova G, Ryzhov V. 1987. Long-term variations of the biogenous elements content and primary production in the Barents Sea waters. In *The Effect of Oceanographic Conditions on Distribution and Population Dynamics of Commercial Fish Stocks in the Barents Sea: Proceedings of the Third Soviet-Norwegian Symposium*, Murmansk, 2–28 May 1986, Loeng H (ed.). Institute of Marine Research: Bergen; 47–58.

NODC. 1994. *World Ocean Atlas*. National Oceanic and Atmospheric Administration, CD-Rom data Sets, Bouldon, Colorado.

Polyak L, Mikhailov V. 1996. Post-glacial environments of the south-eastern Barents Sea: foraminiferal evidence. In *Late Quaternary Palaeoceanography of the North Atlantic Margins*, Andrews JT, Austin WEN, Bergsten H, Jennings AE (eds). Special Publication, Geological Society Publishing House: Bath; 323–337.

Radi T, de Vernal A, Peyron O. 2001. Relationships between dinocyst assemblages in surface sediment and hydrographic conditions in the Bering and Chukchi seas. *Journal of Quaternary Science* **16**: 667–680.

Rey F, Loeng H. 1985. The influence of ice and hydrographic conditions on the development of phytoplankton in the Barents Sea. In *Marine Biology of Polar Regions and Effects of Stress on Marine Organisms*, Gray J, Christiansen M (eds). Wiley: Chichester; 49–63.

Rochon A, de Vernal A. 1994. Palynomorph distribution in Recent sediments from the Labrador Sea. *Canadian Journal of Earth Sciences* **31**: 115–127.

Rochon A, de Vernal A, Turon J-L, Matthiessen J, Head MJ. 1999. *Distribution of dinoflagellates cysts in surface sediments from the North Atlantic Ocean and adjacent basin and quantitative reconstruction of sea-surface parameters*. Contribution Series No. 35, American Association of Stratigraphic Palynologists Foundation: Dallas, Tx.

Rudels B, Jones E, Anderson L, Kattner G. 1994. On the intermediate depth waters of the Arctic Ocean. In *The Polar Oceans and their Role in Shaping the Global Environment*, Johannessen O, Meunch R, Overland J. (eds). American Geophysical Union: Washington; 33–46.

Stager JC, Mayewski PA. 1997. Abrupt early to mid-Holocene climatic transition registered at the equator and the poles. *Science* **276**: 1834–1836.

Stuiver M, Braziunas TF. 1993. Modeling atmospheric ^{14}C influence and ^{14}C marine ages of marine samples to 10 000 BC. *Radiocarbon* **35**: 137–189.

Stuiver M, Reimer PJ, Bard E, Beck JW, Burr GS, Hughen KA, Kromer B, McCormick G, van der Plicht J, Spurk M. 1998. Radiocarbon age calibration, 24 000–0 cal. BP. *Radiocarbon* **40**: 1041–1083.

Stuiver M, Reimer PJ, Reimer R. 2000. *CALIB Radiocarbon Calibration HTML version 4.3 and Marine Reservoir Correction Data Base*. http://depts.washington.edu/qil/calib/.

Velichko A, Andreev A, Klimanov V. 1997. The dynamics of climate and vegetation in the tundra and forest zone during the Late Glacial and Holocene. *Quaternary International* **41/42**: 71–96.

Wright PL. 1974. Recent sediments of the southwestern Barents Sea. *Marine Geology* **16**: 51–81.

Zhang J, Rothrock D, Steele M. 1998. Warming of the Arctic Ocean by a strengthened Atlantic inflow: model results. *Geophysical Research Letters* **25**: 1745–1748.